

1 GSA Data Repository 2017204

doi:10.1130/G38879.1

2
3
4 Small profile concavity of a fine-bed alluvial channel

5
6 **Jongmin Byun^{1,2} and Kyungrock Paik¹**

7 *¹ School of Civil, Environmental, and Architectural Engineering, Korea University, 145*

8 *Anam-ro, Seongbuk-gu, Seoul, 02841, South Korea*

9 *² Department of Civil Engineering and Environmental Sciences, Korea Military Academy*

10 *P.O.Box 77-2, Hwarang-ro, Nowon-gu, Seoul, 01805, South Korea*

11 *email: paik@korea.ac.kr*

12 **θ Range of Natural Streams (Including Both Bedrock and Alluvial Channels)**

13 We collected θ data from a wide range of literature covering both bedrock and alluvial
14 channels. The range spans from 0.11 to 2.1, with mean and standard deviation as 0.63 and
15 0.33, respectively (TABLE DR1).

16 **θ Range of Bedrock Channels at Equilibrium State under Spatially Uniform Uplift Rate**
17 **Regions**

18 We collected θ for bedrock channels, which are reported to be at steady-state under spatially
19 uniform uplift rate region (Snyder et al., 2000; Kirby and Whipple, 2001). Mean and standard
20 deviation are obtained as 0.43 and 0.08 (TABLE DR2).

21 **Ranges and Two Moments of the Scaling Exponents**

22 Two process parameters α and β are known to range mostly between 1 and 2 (Prosser and
23 Rustomji, 2000; Peckham, 2003; Paik, 2012). For their distributions, we adopted $\mu_\alpha=\mu_\beta=1.5$
24 and $\sigma_\alpha=\sigma_\beta=0.25$. Recall that we have three geomorphic parameters (n , h , and p) originated
25 from aforementioned scaling relationships. For n , we used $\mu_n=0.0667$ and $\sigma_n=0.0135$, given
26 by Parker et al. (2007). h is empirically found to be between 0.5 and 0.7 (Hack, 1957; Gray,
27 1961; Robert and Roy, 1990; Crave and Davy, 1997). Here, $\mu_h=0.6$ and $\sigma_h=0.05$ were used. p
28 varies between 0.3 and 0.9 (Brierley and Hickin, 1985) (TABLE DR3), and we adopted
29 $\mu_p=0.6$ and $\sigma_p=0.2$. Finally, the last parameter of γ is typically less than 1 but no less than 0.5
30 when it comes to the dominant discharge. We used $\mu_\gamma=0.77$ and $\sigma_\gamma=0.09$, estimated from
31 literature (TABLE DR4). Physically unrealistic parameter ranges, i.e., $\alpha < 0$, $\beta < 0$, $\gamma < 0$, $\gamma >$
32 1 , $h < 0$, and $p < 0$, were truncated from the Gaussian distributions.

33 **Analysis of Four Alluvial Rivers**

34 Longitudinal profiles and area-slope relationships have been extracted from DEM for the
35 Minnesota and the Sugar-Wabash Rivers in Midwest USA (Figure DR1). The same analysis
36 was repeated for the Gwda-Noteć (Poland) and the Neman (Lithuania) Rivers in northern
37 Europe (Figure DR2). The analysis was implemented using TopoToolbox (Schwanghart and
38 Kuhn, 2010) software in the following procedure. *Italic terms in parentheses are the name of*
39 *functions in TopoToolbox.*

40 **(A) Preprocessing DEM**

41 We first filled sinks (depression cells) in the DEM (*fillsinks*). Then flow directions were
42 assigned based on the D8 algorithm (*FLOWobj*) and flow accumulation was calculated
43 (*flowacc*) on the filled DEM, sequentially.

44 **(B) Selection of channel reaches**

45 In this analysis, we defined a DEM cell of which upslope area equals 100 cells
46 (approximately 0.64 km²) as channel head. This criterion has been consistently applied for
47 four study rivers. Accordingly, flow paths extracted from DEM are pruned (*STREAMobj*) and
48 specific reaches for which longitudinal profiles are extracted were selected (*modify*).

49 **(C) Drawing longitudinal profiles**

50 Longitudinal profiles were drawn for each selected reach (*plotdz*). Raw DEM was used in the
51 drawing and hence sinks are shown in profiles (Figure 3). The sink-filled DEM was only
52 used for flow direction extraction.

53 **(D) Plotting area-slope relationships**

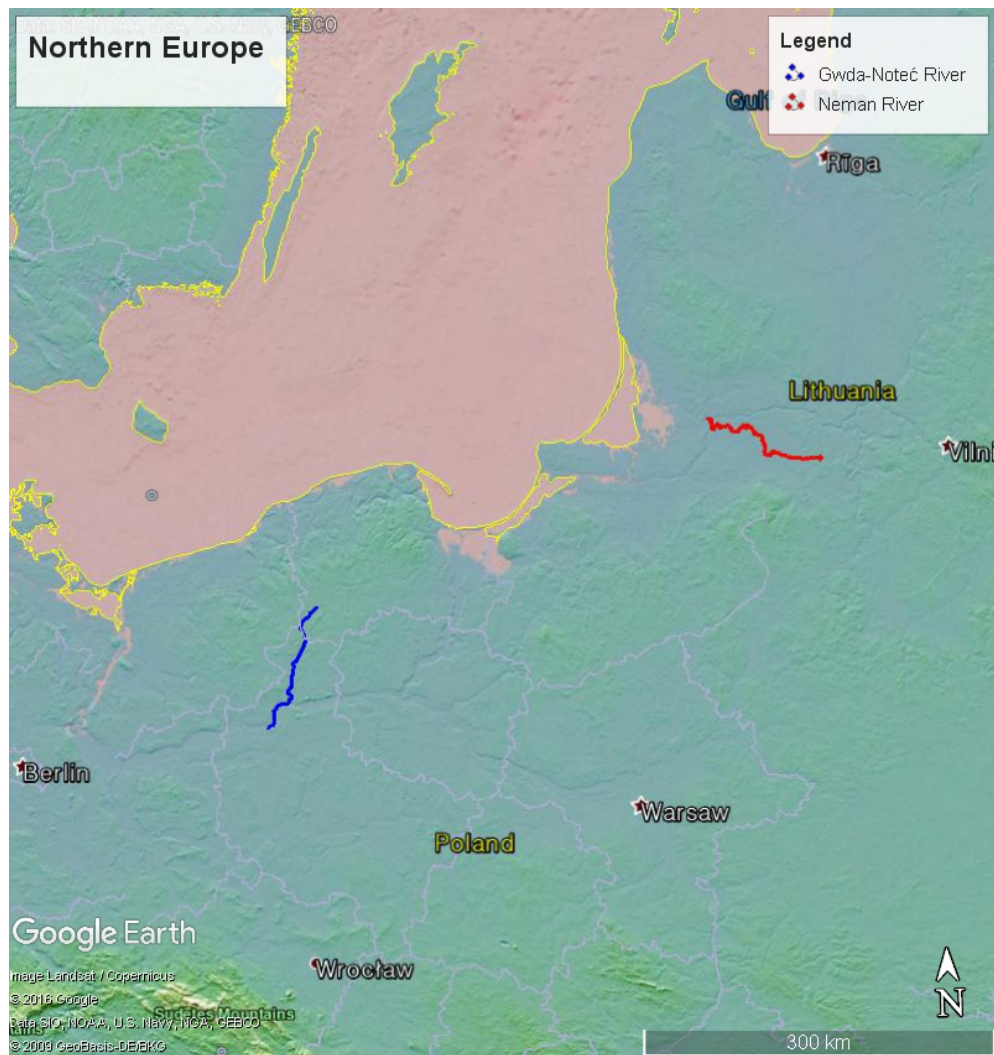
54 Local slope at each cell was calculated with the distance to the downstream cell of 30 m
55 vertical drop (*slopearea* with ‘drop’ option). After a couple of trial-and-error, this criterion
56 was found appropriate to prevent negative slope due to sinks in DEM. This criterion was
57 consistently used for all four study rivers.

58 **Figure**



59

60 **Figure DR1. Location of the Minnesota and the Sugar-Wabash Rivers in Midwest USA**



61

62 Figure DR2. Location of the Gwda-Noteć (Poland) and the Neman (Lithuania) Rivers in
63 northern Europe

TABLE DR1. PROFILE CONCAVITY DATA FROM LITERATURE.

Location	θ
Middle River, Appalachians, Virginia (three branches)*	0.64, 0.59, 0.49
North River, Appalachians, Virginia (four branches)*	0.43, 0.47, 0.56, 0.52
Montgomery Fork, Tennessee†	0.37
Watson Creek, Ohio†	0.58
Left Fork, Washington and Virginia†	0.78
Grovers Creek, Kentucky†	0.52
Bear Branch, Kentucky†	0.65
Cooks Run, Pennsylvania†	0.56
Hawes Fork, Kentucky†	0.83
West Bays Fork, Kentucky†	0.40
Flat Creek, Kentucky†	0.63
McGills Creek, Kentucky†	0.59
Brush Run, Pennsylvania†	0.70
Virginia Badlands§	0.15
Utah Badlands§	0.19
Great Plains§	0.20
Ephemeral, New Mexico (two channels)§	0.15, 0.11
Walnut Gulch, Arizona (three sub-basins)‡	0.30, 0.29, 0.25
Big Creek, Idaho (two sub-basins)#	0.51, 0.48
North Fork Cour d'Alene River, Idaho#	0.47
St. Joe River, Idaho (two sub-basins)#	0.47, 0.56
St. Regis River, Montana (two sub-basins)#	0.55, 0.55
Schoharie Creek, New York (three sub-basins)#	0.48, 0.42, 0.43
East Delaware River, New York#	0.55
Racoon Creek, Pennsylvania (two sub-basins)#	0.51, 0.34
Beaver Creek, Pennsylvania and Ohio#	0.34
Buck Creek, northern California‡	0.48
Brushy Creek, Alabama#	0.53
Moshannon Creek, Pennsylvania#	0.58
Montgomery Fork, Tennessee‡	0.85
Siuslaw, Umpqua, and Alsea River basins, southern coastal Oregon**	1.00
Mahantango Creek, Pennsylvania††	0.49
Central Zagros Mountains, Iran††	0.42
Upper Noyo River, California (seven sub-basins)§§	0.89, 0.56, 0.65, 0.83, 1.13, 0.59, 0.67
Coastal basins, northern California (21 basins)###	0.37, 0.29, 0.58, 0.43, 0.45, 0.44, 0.41, 0.40, 0.58, 0.25, 0.36, 0.39, 0.31, 0.47, 0.42, 0.37, 0.52, 0.48, 0.46, 0.59, 0.36
Waipaoa River, New Zealand (five sub-basins)***	0.61, 0.53, 0.49, 0.55, 0.57
Southern Sierra Madre Occidental, Mexico (11 rivers)†††	0.24, 0.52, 0.63, 0.35, 0.74, 0.53, 0.42, 0.53, 0.35, 0.85, 0.19
Santa Ynez Mountains, coastal California (50 channels)§§§	0.58, 0.35, 0.48, 0.41, 0.67, 0.53, 0.40, 0.34, 0.97, 0.51, 1.60, 0.65, 0.62, 1.10, 0.87, 0.85, 0.74, 0.87, 1.80, 2.10, 0.89, 0.72, 0.86, 0.92, 0.54, 0.60, 0.55, 0.38, 1.20, 0.71,

	0.40, 1.90, 1.60, 1.20, 0.90, 0.76, 0.58, 0.97, 0.81, 0.77, 0.88, 0.69, 0.54, 0.55, 0.37, 0.56, 0.54, 0.55, 0.58, 1.00
Eastern Central Range, Taiwan (16 rivers) ^{####}	0.77, 0.78, 0.72, 1.54, 1.41, 1.30, 0.54, 1.01, 0.96, 0.78, 0.94, 0.90, 0.65, 0.95, 0.95, 0.52

* Hack (1957). For the calculated θ values, refer to Tucker and Whipple (2002).

† Flint (1974).

§ Howard (1980). Each θ was calculated assuming that Hack's exponent is 0.6.

Tarboton et al. (1991).

** Seidl and Dietrich (1992).

†† Tucker (1996). Refer to Tucker and Whipple (2002).

§§ Sklar and Dietrich (1998)

Snyder et al. (2000).

*** Whipple and Tucker (2002).

††† Montgomery and López-Blanco (2003)

§§§ Duvall et al. (2004).

Stolar et al. (2007).

AREAS.

Location and Reference	Fitted θ
<i>Basin names of the measured channels in the Mendocino triple junction region, northern California (Snyder et al., 2000)</i>	
Singley	0.37
Davis	0.29
Fourmile	0.58
Cooskie	0.43
Randall	0.45
Spanish	0.44
Oat	0.41
Kinsey	0.40
Big	0.58
Big Flat	0.25
Shipman	0.36
Buck	0.39
Gitchell	0.31
Horse Mtn.	0.47
Telegraph	0.42
Whale	0.37
Jackass	0.52
Hardy	0.48
Juan	0.46
Howard	0.59
Dehaven	0.36
Davis	0.43
<i>Channels in the Siwalik Hills in central Nepal* (Kirby and Whipple, 2001)</i>	
14	0.50
15	0.47
16	0.48
17	0.51
18	0.44
19	0.34
20	0.51
<u>Averaged θ value</u>	0.43\pm0.08
* Data for only the bedrock channels flowing parallel to the strike of the anticline, thereby under the spatially uniform uplift rate regions. Numbers refer to channels in Kirby and Whipple (2001)'s Data Repository Table DR1 and Figure DR1.	

70 TABLE DR3. REPORTED p VALUES FOR THE POWER FUNCTIONAL DOWNSTREAM FINING EQUATION (THE SQUAMISH RIVER, CANADA,
 71 FITTED WITH MEDIAN GRAIN SIZE) (Brierley and Hickin, 1985)

Location and Type	p
Braided Reach	0.79
Meandering Section	0.76
Within the Canyon	0.38

72

73

TABLE DR4. REVIEWED RELATIONS BETWEEN DISCHARGE OF A GIVEN FREQUENCY OF OCCURRENCE AND UPSTREAM CONTRIBUTING

74

AREA ($Q^\infty A^r$)

γ	Corresponding flow frequency	Location and Reference
~1	Average annual discharge	Potomac River basin, USA (Hack, 1957)
0.895	Bankfull discharge	High-elevation basins in Colorado, USA (Segura and Pitlick, 2010)
0.85	Mean annual flood discharge ($Q_{2.33}$)	New England, USA (Benson, 1962)*
0.80	Mean annual flood discharge ($Q_{2.33}$)	Pennsylvania, USA (Brush, 1961)
0.78	Mean annual flood discharge ($Q_{2.33}$)	River Trent, England (Knighton, 1987)*
0.77	Mean annual flood discharge ($Q_{2.33}$)	British Isles, (NERC, 1975)*
0.74	Mean annual flood discharge ($Q_{2.33}$)	Great Britain, (Nash and Shaw, 1966)*
0.70	Annual maximum flood peak discharge	Pennsylvania and New Jersey, USA (Aron and Miller, 1978) [†]
0.62	Average annual peak discharge	Kentucky, USA (Sólyom and Tucker, 2004)
0.57	~90th Percentile unit discharge [§]	USA and Puerto Rico, (O'Connor and Costa, 2004)
0.53	~99th Percentile unit discharge [§]	USA and Puerto Rico, (O'Connor and Costa, 2004)

* Cited in Knighton (1999).

[†] Cited in Snow and Slingerland (1987).[§] Peak discharge divided by drainage area.

75

REFERENCES CITED

- Brierley, G.J., and Hickin, E.J., 1985, The downstream gradation of particle sizes in the Squamish river, British Columbia: *Earth Surface Processes and Landforms*, v. 10, no. 6, p. 597–606.
- Crave, A., and Davy, P., 1997, Scaling relationships of channel networks at large scales: Examples from two large-magnitude watersheds in Brittany, France: *Tectonophysics*, v. 269, p. 91–111, doi:10.1016/S0040-1951(96)00142-4.
- Duvall, A., Kirby, E., and Burbank, D., Tectonic and lithologic controls on bedrock channel profiles and processes in coastal California: *Journal of Geophysical Research: Earth Surface*, v. 109, no. F3, F03002.
- Flint, J.J., 1974, Stream gradient as a function of order, magnitude, and discharge: *Water Resources Research*, v. 10, no. 5, p. 969–973.
- Gray, D.M., 1961, Interrelationships of watershed characteristics: *Journal of Geophysical Research*, v. 66, p. 1215–1223, doi:10.1029/JZ066i004p01215.
- Hack, J.T. 1957, Studies of longitudinal stream profiles in Virginia and Maryland, U. S. Geological Survey Professional Paper, 294B.
- Howard, A.D., 1980, Thresholds in river regimes: Thresholds in geomorphology, p. 227–258.
- Kirby, E., and Whipple, K., 2001, Quantifying differential rock-uplift rates via stream profile analysis: *Geology*, v. 29, p. 415–418.
- Knighton, A.D., 1999, Downstream variation in stream power: *Geomorphology*, v. 29, p. 293–306.
- Montgomery, D.R., and López-Blanco, J., 2003, Post-Oligocene river incision, southern Sierra Madre Occidental, Mexico: *Geomorphology*, v. 55, p. 235–247.
- Paik, K., 2012, Simulation of landscape evolution using a global flow path search method: *Environmental Modelling & Software*, v. 33, p. 35–47, doi:10.1016/j.envsoft.2012.01.005.
- Parker, G., Wilcock, P.R., Paola, C., Dietrich, W.E., and Pitlick, J., 2007, Physical basis for quasi-universal relations describing bankfull hydraulic geometry of single-thread gravel bed rivers: *Journal of Geophysical Research*, v. 112, F04005, doi: 10.1029/2006JF000549.
- Peckham, S.D., 2003, Fluvial landscape models and catchment-scale sediment transport: *Global and Planetary Change*, v. 39, p. 31–51, doi:10.1016/S0921-8181(03)00014-6.
- Prosser, I.P., and Rustomji, P., 2000, Sediment transport capacity relations for overland flow: *Progress in Physical Geography*, v. 24, p. 179–193, doi:10.1191/030913300669852483.

111 Robert, A., and Roy, A.G., 1990, On the fractal interpretation of the mainstream
 112 length-drainage area relationship: *Water Resources Research*, v. 26, p. 839–842,
 113 doi:10.1029/WR026i005p00839.

114 Schwanghart, W., and Kuhn, N.J., 2010, TopoToolbox: A set of Matlab functions for
 115 topographic analysis: *Environmental Modelling & Software*, v. 25, issue 6, p.
 116 770-781, doi:10.1016/j.envsoft.2009.12.002.

117 Segura, C., and Pitlick, J., 2010, Scaling frequency of channel-forming flows in
 118 snowmelt-dominated streams: *Water Resources Research*, v. 46, no. 6, W06524.

119 Seidl, M.A., and Dietrich, W.E., 1992, The problem of channel erosion into bedrock. In:
 120 Schmidt, K.H., de Ploey, J. (Eds.), *Functional Geomorphology: Landform Analysis*
 121 *and Models*, Catena Supplement, v. 23, p. 101-124.

122 Sklar, L., and Dietrich, W.E., 1998, River longitudinal profiles and bedrock incision models:
 123 Stream power and the influence of sediment supply. In: Tinkler, K., Wohl, E. (Eds.),
 124 *Rivers over rock: Fluvial processes in Bedrock channels*, *Geophysical Monograph*, v.
 125 107, p. 237-260.

126 Snow, R.S., and Slingerland, R.L., 1987, Mathematical modeling of graded river profiles:
 127 *Journal of Geology*, v. 95, p. 15–33.

128 Snyder, N.P., Whipple, K.X., Tucker, G.E., and Merritts, D.J., 2000, Landscape response to
 129 tectonic forcing: Digital elevation model analysis of stream profiles in the Mendocino
 130 triple junction region, Northern California: *Bulletin of the Geological Society of*
 131 *America*, v. 112, p. 1250–1263.

132 Stolar, D.B., Willett, S.D., and Montgomery, D.R., 2007, Characterization of topographic
 133 steady state in Taiwan: *Earth and Planetary Science Letters*, v. 261, p. 421-431.

134 Tarboton, D.G., Bras, R.L., and Rodriguez-Iturbe, I., 1991, On the extraction of channel
 135 networks from digital elevation data: *Hydrological Processes*, v. 5, p. 81–100.

136 Tucker, G.E., and Whipple, K.X., 2002, Topographic outcomes predicted by stream erosion
 137 models: Sensitivity analysis and intermodel comparison: *Journal of Geophysical*
 138 *Research B: Solid Earth*, v. 107, no. B9, 2179.

139 Whipple, K.X., and Tucker, G.E., 2002, Implications of sediment-flux-dependent river
 140 incision models for landscape evolution: *Journal of Geophysical Research B: Solid*
 141 *Earth*, v. 107, p. ETG 3–1–ETG 3–20, doi:10.1029/2000JB000044.